ISIJ International, Vol. 38 (1998), No. 6, pp. 572–579

Effect of Carbon on the Cold-worked State and Annealing Behavior of Two 18wt%Cr–8wt%Ni Austenitic Stainless Steels

Luis Fernando Maffeis MARTINS, Ronald Lesley PLAUT[1)] and Angelo Fernando PADILHA[1)]

Mangels - Steel Division, 09895-900, São Bernardo do Campo, Brazil. 1) Department of Materials and Metallurgical Engineering, University of São Paulo, 05508-900, São Paulo, Brazil.

(Received on August 25, 1997; accepted in final form on November 18, 1997)

The influence of carbon on the work hardening, formation and reversion of deformation induced martensite and on the recrystallization of two austenitic stainless steels 18%Cr–8%Ni type were studied with the help of different microstructural analysis techniques. Two steels were selected: the first an AISI 304L with low carbon (%C = 0.021) content and the second an AISI 304 with higher carbon (%C = 0.065) content. Both steels were heat treated to obtain two different initial conditions: one with the carbon completely in solid solution (after a solution annealing treatment at 1 100°C) and the other with practically all the carbon in the precipitated form, as $(Cr,Fe)_{23}C_6$ (after a precipitation treatment at 750°C). The material having higher carbon content, both in solid solution and precipitated, presented in both cases higher strain hardening, smaller tendency to form strain induced martensite and higher resistance to recrystallization. Carbon in solid solution, as compared to the precipitated condition, led to a material with a higher tendency to strain hardening, less susceptibility to martensite formation and more resistance to recrystallization. Nucleation of recrystallization preferably occurred in the vicinity of grain boundaries. Based on the results of the kinetics of recrystallization and intergranular corrosion tests it was concluded that the usually recommended annealing temperatures (1 000 to 1 120°C) are sometimes unnecessarily high.

KEY WORDS: austenitic stainless steels; work hardening; strain induced martensite; recovery; recrystallization.

1. Introduction

Carbon has a major role in austenitic stainless steels. In solid solution, it stabilizes austenite and increases the strength *via* solid solution hardening. Around 1 100°C, it is possible to dissolve more than 0.1 wt% C in an AISI 316 steel and at about 750°C the solubility drops to less than 50 ppm.[1)] In the majority of cases, carbon is undesirable in this type of steels, because it precipitates preferentially at grain boundaries as $(Cr,Fe,Mo)_{23}C_6$, leading to chromium depletion in adjacent regions, making the steel susceptible to intergranular corrosion. Further, the depletion of chromium promotes, during cooling, the formation of α'-martensite (BCC, ferromagnetic) formation within near-grain boundary regions.[2)] The formation of α' during cooling can be attributed to the increase of the Ms temperature above room temperature due to changes in composition caused by carbide precipitation during aging.[3)]

Austenitic stainless steels show significant hardening after cold working. This behavior has been attributed to the low stacking fault energies (SFE) of this type of steels[4,5)] and to the formation of strain induced α'-martensite.[6,7)] The tendency to work harden increases with decreasing nickel content or increasing carbon content.

Apart from recovery and recrystallization, it can also be observed on annealing of the strain hardened material, martensite reversion[8–10)] and eventually some $M_{23}C_6$ precipitation. The precipitation that occurs during annealing of cold worked supersaturated solid solutions can delay their recrystallization.[11)]

The objective of this work is to study the influence of carbon on (i) the work hardening behavior; (ii) the formation and reversion of strain induced martensite and (iii) recrystallization of austenitic stainless steels of the 18wt%Cr–8wt%Ni type. Therefore, two types of steels were selected; the AISI 304L, having 0.021 wt% C, and the AISI 304, having 0.065 wt% C. Both steels were heat treated to obtain two initial conditions: carbon completely in solid solution (after a solution annealing at 1 100°C) and carbon nearly completely precipitated as $(Cr,Fe)_{23}C_6$ (after a precipitation heat treatment at 750°C).

2. Experimental Procedure

Samples of AISI 304 and AISI 304L were received as sheets with 1.5 mm thickness. The final processing stages were cold rolling followed by annealing. Chemical compositions are given in **Table 1**.

Samples of both steels were initially solution annealed at 1 100°C for 1 h followed by water cooling (designation S). After solution annealing, steels AISI 304 and 304L presented an average grain size of 157 and 85 μm, respectively. Half of the solubilized samples were submitted to precipitation aging at 750°C for 24 h (designation S + P).

Two rolling mills were used in this work. For the determination of the work hardening curves (hardness *versus* thickness reduction) and the α'-martensite for-

Table 1. Chemical composition of AISI 304 and AISI 304L. (wt%)

	C	Cr	Ni	Mn	Si	N	P	S
AISI 304	0.065	18.12	8.37	1.35	0.48	0.0464	0.025	0.002
AISI 304L	0.021	18.44	9.38	1.37	0.56	0.0383	0.026	0.004

mation curves (α'-martensite % *versus* thickness reduction) it was used a very precise laboratorial rolling mill. On the other hand, for the annealing experiments the specimens were cold rolled in an industrial equipment.

The samples were cold rolled with reductions of 10 to 60%. These samples were subsequently annealed at temperatures of 500, 550, 650, 700, 750, 850, 900, 950, and 1 000°C for 1 h. The samples having a 60% cold reduction were submitted to 12 isothermal annealing cycles at 750°C with times ranging from 5 min to 24 h.

Several complementary microstructural analysis techniques were employed: optical microscopy (OM), scanning electron microscopy (SEM), energy dispersive analysis (EDX), transmission electron microscopy (TEM), X-ray diffraction (XRD), phase magnetic detection (PMD) and hardness measurements.

Two metallographic etchants were utilized:

a) V2A-etchant (20 and 40 sec immersion): 100 m*l* hydrochloric acid, 10 m*l* nitric acid, 100 m*l* water, 0.3 m*l* special etchant.[12]

b) 30% nitric acid in water, electrolytic (0.5 and 1.0 V for approx. 5 min).

The V2A-etchant, combined with polarized light and interference contrast, was used to analyze the cold worked and the partially recrystallized samples. The second etchant was employed for the determination of the grain size in recrystallized samples. Depending on time and mainly on the voltage utilized this etchant reveals only grain boundaries and does not reveal coherent twins boundaries.[13]

The SEM was employed mainly to detect the presence, quantity, size, morphology and distribution of the $(Cr,Fe)_{23}C_6$ carbide. Samples were analyzed after etching with the V2A-etchant. The EDX linked to the SEM was used to determine the metallic content of the phases.

The TEM was used to study the substructure of crystal defects, mainly dislocations arrangements of the cold worked samples after annealing. Sample preparation was carried out by careful thinning with #1 000 emery paper down to a thickness of 130 to 180 μm, coining out of 3 mm disks and subsequent thinning by electrolytic polishing with double jets. The electrolyte used was a A7 Struers, with the following composition: 700 m*l* methanol, 200 m*l* glicerol and 100 m*l* perchloric acid. The electrolyte was kept at −20°C and 30 V. Electrolytic polishing was done on a Struers Tenupol-3 equipment. Observations were carried out on a Philips CM 20 microscope operating at 200 kV.

X-ray diffractions were obtained with a PW 1710 Phillips diffractometer with a $CuK_{\alpha 1}$ ($\lambda = 0.15405$ nm) radiation.

The determination of eventual magnetic phases, in the present case α'-martensite, was done on a Fisher ferritoscope. This equipment has a 0.1% ferrite detection limit.

Hardness measurements, used in the determination of hardening and softening curves, were made with a 10 kg load.

The softening (S) of a sample X was calculated as being given by:

$$S = (Hw - Hx)/(Hw - Hr) \cdot 100$$

where Hw and Hr are the hardness of the cold worked and recrystallized conditions, respectively, and Hx is the hardness of the X sample.

Intergranular corrosion resistance of the recrystallized samples was evaluated with the oxalic acid technique, in accordance to practice A—ASTM A 262 and W of ASTM A 763 standards.

3. Results and Discussion

Results will be presented and discussed in the following sequence: strain hardening, α'-martensite formation, α'-reversion, recrystallization initiation sites (nucleation), recrystallization kinetics, recrystallized grain size, and intergranular corrosion.

Figure 1 presents the micrographs obtained on the SEM for both steels studied, after solution annealing at 1 100°C (Figs. 1a) and 1b)) and after precipitation at 750°C for 24 h (Figs. 1c) and 1d)).

3.1. Strain Hardening

In the solubilized condition, steel AISI 304 presents higher strain hardening than the AISI 304L steel (see **Fig. 2a)**). In the AISI 300 series, there is an inverse relationship between the stacking fault energy (SFE) and the Cr/Ni ratio.[4,5] In other words, the higher the Cr/Ni ratio, the smaller will be the SFE. The Cr/Ni ratios for both steels in this work, in the solubilized condition, are 2.16 and 1.97, respectively. Furthermore, the AISI 304 has 3 times more carbon in solid solution than the AISI 304L. Therefore, it is expected that the AISI 304 steel, having lower SFE and larger amounts of interstitials in solid solution, would have a more pronounced strain hardening as compared to the AISI 304L steel.

In the precipitated condition, steel AISI 304 also presents higher strain hardening than the AISI 304L (see **Fig. 2b)**). In this case, the carbon content in solid solution is practically nil in both steels. On the other hand, the AISI 304 steel presents a larger quantity of carbide precipitates, preferentially on grain and on incoherent twin boundaries. The $(Cr,Fe)_{23}C_6$ precipitation may cause chrome depletion in the matrix and reduction in the Cr/Ni ratio. Supposing that all carbon of both steels precipitates with the stoichiometry $Cr_{23}C_6$, the new values of the Cr/Ni ratio for both steels would be 2.04 and 1.93, respectively. Hence, in this case, it is expected that steel AISI 304, with lower SFE and larger amount of precipitates, would present higher strain hardening than AISI 304L steel.

It remains to be discussed if the carbon is more effective on strain hardening when it is in solid solution than when it is precipitated in the chrome carbide form. The analysis of **Figs. 2c)** and **2d)** shows that carbon is more effective when in solid solution, although the differences observed in this work were not large. There are some reasons

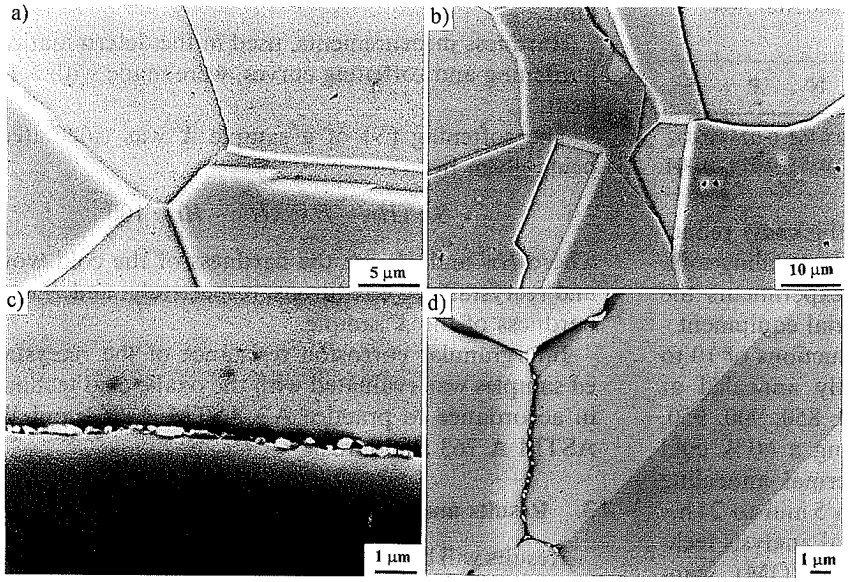

Fig. 1.
AISI 304 and AISI 304L steels after solution annealing at 1100°C (a) and b)), and after precipitation at 750°C for 24 h (c) and d)). SEM secondary-electron images after V2A etching.

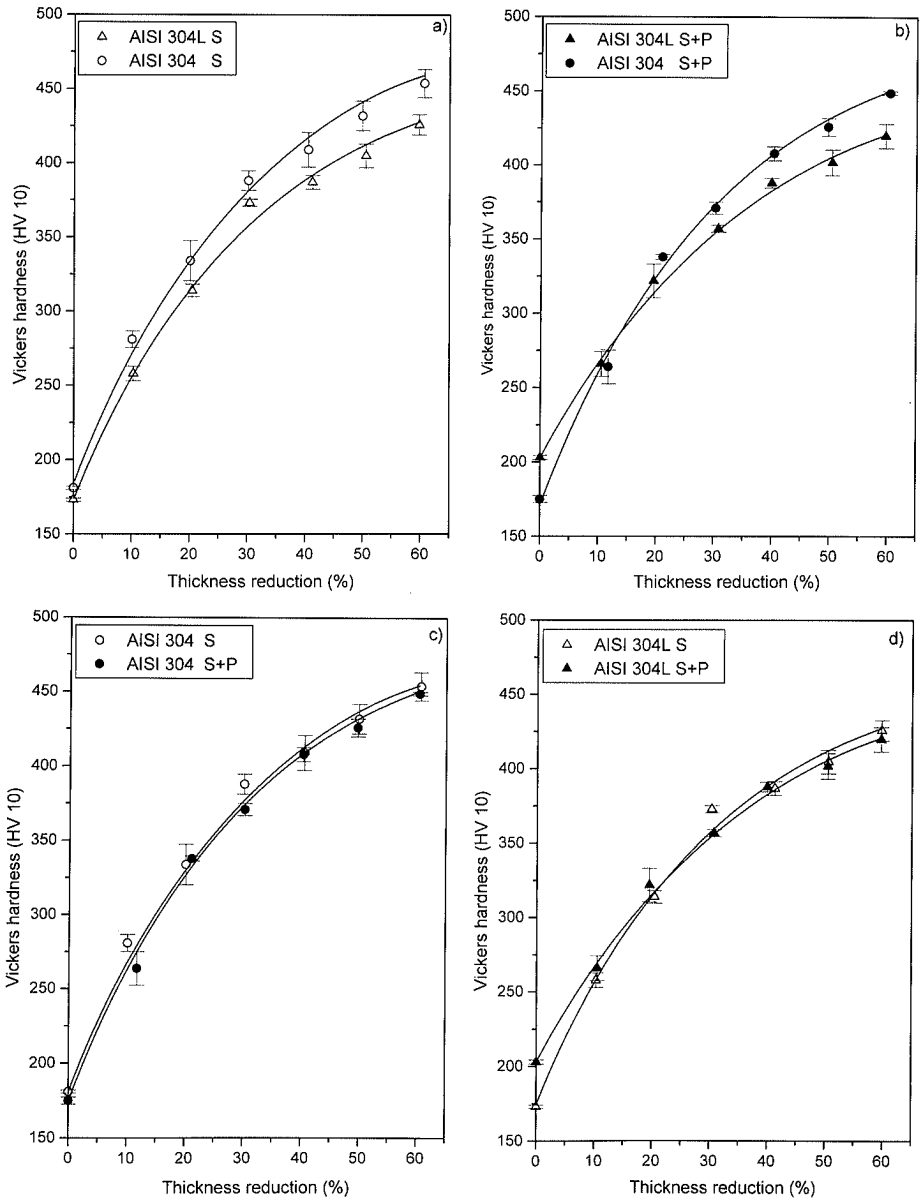

Fig. 2.
Vickers hardness curves (10 kg load) *vs.* thickness reduction. (%)
a) AISI 304 and AISI 304L steels; initially solubilized (S) condition.
b) AISI 304 and AISI 304L steels; initially solubilized and precipitated (S+P) condition.
c) AISI 304 steel; initially solubilized (S), and precipitated (S+P) conditions.
d) AISI 304L steel; initially solubilized (S), and precipitated (S+P) conditions.

for this behavior: the $(Cr,Fe)_{23}C_6$ carbides preferably precipitate on grain and twin boundaries, *i.e.*, it is non-uniform, therefore causing insignificant additional strain hardening and also reduction of the Cr/Ni ratio in the matrix, increasing the SFE. In general, alloys with uniform fine and incoherent particle distribution, show

an accentuated strain hardening (Orowan mechanism). In the case of stainless steels, the $M_{23}C_6$ precipitation is very localized in the form of a carbide network on the grain boundaries and the additional strain hardening hence obtained is insignificant.

3.2. Formation of Strain Induced Martensite

Although the AISI 304 steel showed higher strain hardening than the AISI 304L, as discussed in Sec. 3.1, the AISI 304L steel presented higher susceptibility to the formation of strain induced α'-martensite (see **Figs. 3a)** and **3b)**).

To analyze the tendency toward the formation of strain induced martensite it is convenient to calculate the Md values. Using, for example, the formulation proposed by Angel[14] and the composition given in Table 1, the temperatures of 15.3 and 25.5°C are obtained for the AISI 304 and AISI 304L steels, respectively. Hence, the greater tendency toward α'-martensite formation in the AISI 304L steel is justified by its composition, which in turn, implies in a higher Md value. In this case (Fig. 3a)), it was supposed that all carbon was in solid solution.

By comparing both steels in the precipitated condition, the new values of Md are 60.1 and 40°C for the AISI 304 and AISI 304L steels, respectively. In other terms, the matrix composition changes due to precipitation suggests that the AISI 304 steel be more susceptible to strain induced α'-martensite formation than the AISI 304L steel, exactly the opposite to what was experimentally observed (Fig. 3b)). The modifications in chemical analysis caused by precipitation are restricted to the vicinity of grain and twin boundaries, whilst the calculated values obtained by the formula suppose that the chrome depletion has occurred homogeneously throughout the entire volume. The chrome depletion in the boundary vicinity is so accentuated that it causes the formation of α'-martensite on cooling and in the absence of deformation (Fig. 3b)). In the grain interior there is practically no chrome depletion.

No ε-martensite (HCP, non-magnetic) was detected in the present work. An explanation for this is that at the high strains employed, ε-martensite, that might be

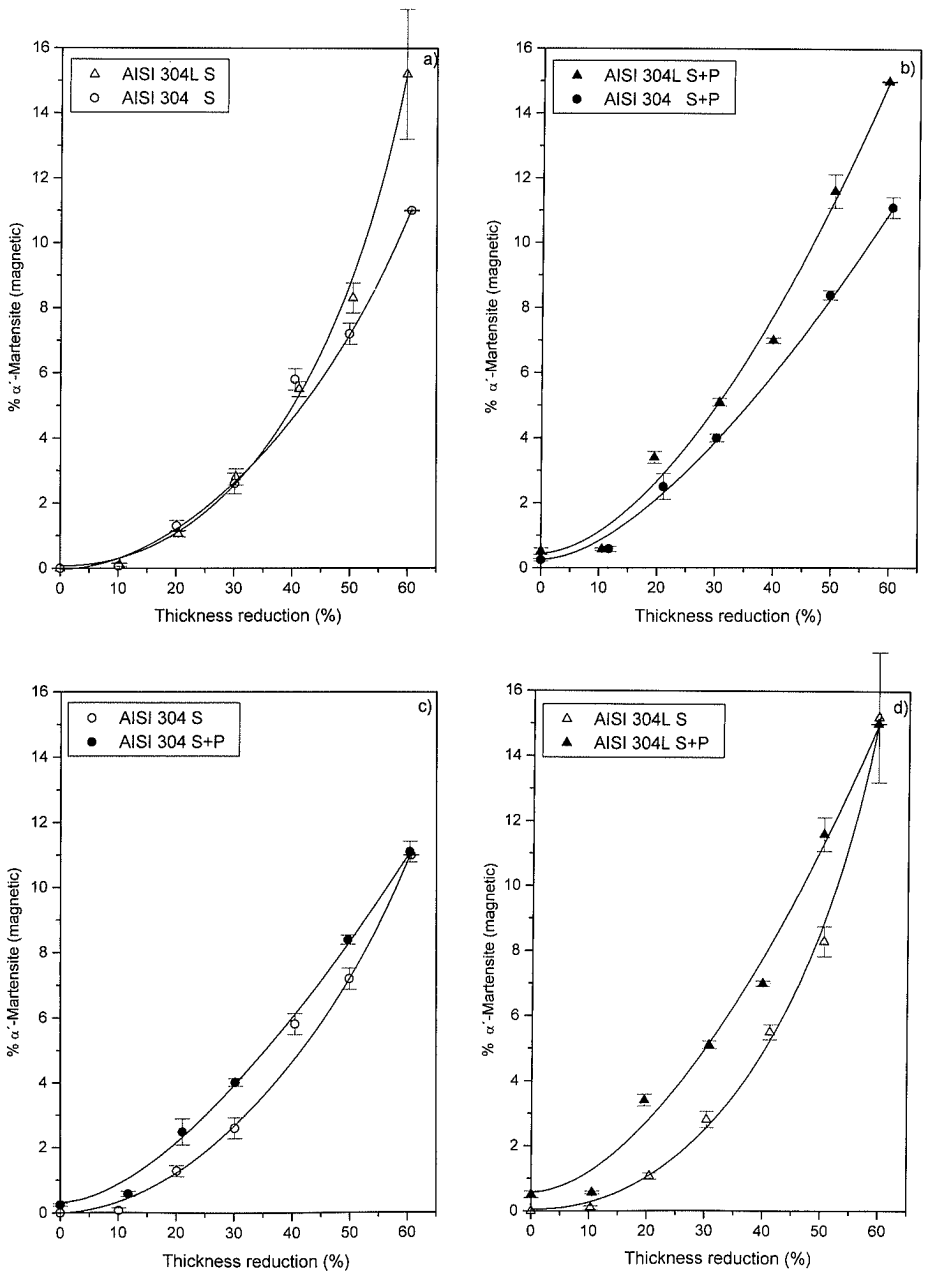

Fig. 3.
Martensite % *vs.* thickness reduction %.
a) AISI 304 and AISI 304L steels; initially solubilized (S) condition.
b) AISI 304 and AISI 304L steels; initially solubilized and precipitated (S+P) condition.
c) AISI 304 steel; initially solubilized (S) and precipitated (S+P) conditions.
d) AISI 304L steel; initially solubilized (S) and precipitated (S+P) conditions.

eventually formed, would be already transformed to α'-martensite. Another explanation is that the absence of ε-martensite indicates that the deformation mode is the sequence: $\gamma \rightarrow$mechanical twin $(\gamma') \rightarrow \alpha'$-martensite, rather than the sequence $\gamma \rightarrow \varepsilon$-martensite $\rightarrow \alpha'$-martensite.[15]

Finally, it should be pointed out that the precipitation of $M_{23}C_6$ makes the material susceptible to the α' formation (see **Figs. 3c)** and **3d)**). However, this effect tends to disappear at reductions of about 60%.

3.3. The α'-reversion

α'-reversion temperature revealed small sensitivity to the type of steel, to the strain level and to the initially different heat treatment conditions. From **Figs. 4a)** to **4d)**, it is possible to determine a 50% reversion temperature ($T_{50\%RM}$). For the 12 studied conditions (2 steels × 2 heat treatments × 3 strain levels), the $T_{50\%RM}$ temperature is about 550 ± 20°C. This temperature range is below the recrystallization temperature, as will be discussed in the next items. Furthermore, its kinetics is faster than the recrystallization. For example, at 750°C, the α'-reversion was nearly complete after 5 min treatment.

3.4. Recrystallization Initiation Sites

In general, the nucleation (recrystallization initiation) occurs preferentially at the vicinity of grain boundaries, and on deformation bands.

It is interesting to mention that in the precipitated condition the "old" (prior) grain boundaries stay practically immobilized by the precipitates. Even then, the recrystallization nucleation occurs preferentially in the vicinities of grain boundaries, because in these locations the heterogeneous deformation must be more pronounced. The heterogeneity is caused by the differences in orientation in neighboring grains and by the presence of precipitates.

3.5. Kinetics of Recrystallization

A general analysis of the softening curves **(Figs. 5a)** and **5b)**), allows the conclusion that the presence of

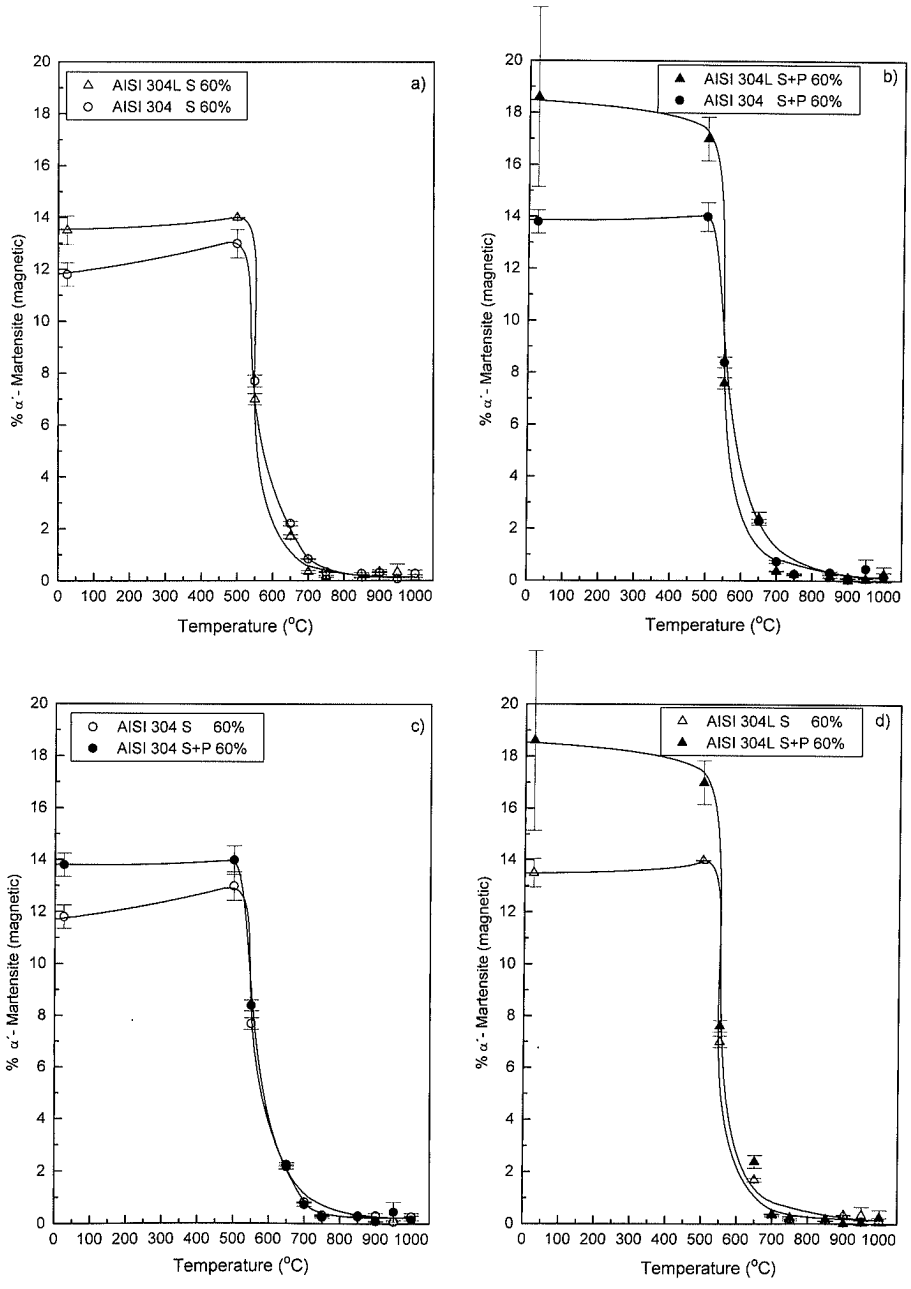

Fig. 4.
Martensite reversion curves (% martensite *vs.* annealing temperature - 1 h).
a) AISI 304 and AISI 304L steels; initially solubilized (S) condition.
b) AISI 304 and AISI 304L steels; initially solubilized and precipitated (S+P) condition.
c) AISI 304 steel; initially solubilized (S) and precipitated (S+P) conditions.
d) AISI 304L steel; initially solubilized (S) and precipitated (S+P) conditions.

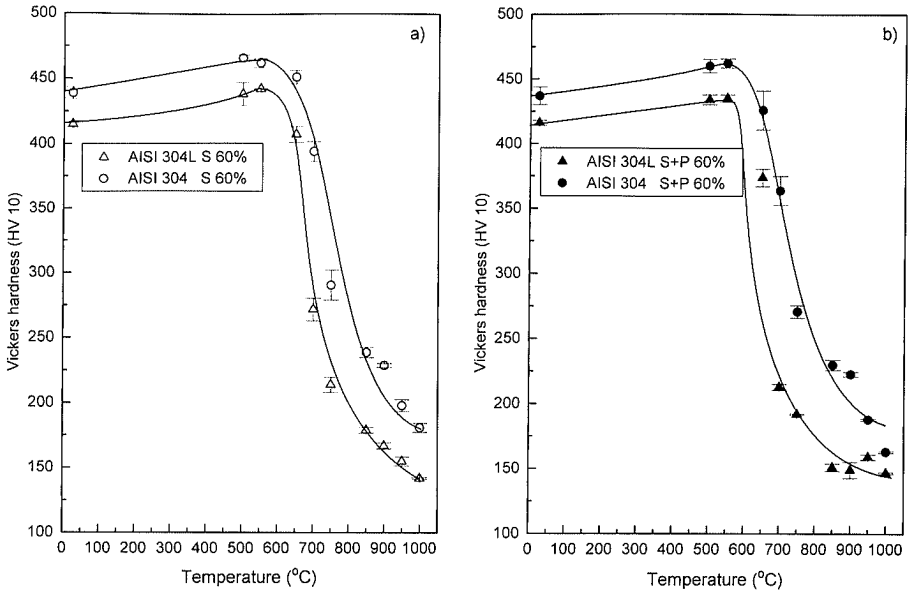

Fig. 5.
Softening curves (Vickers hardness-10 kg load *vs.* annealing temperature - 1 h).
a) AISI 304 and AISI 304L steels; initially solubilized (S) condition.
b) AISI 304 and AISI 304L steels; initially solubilized and precipitated (S + P) condition.

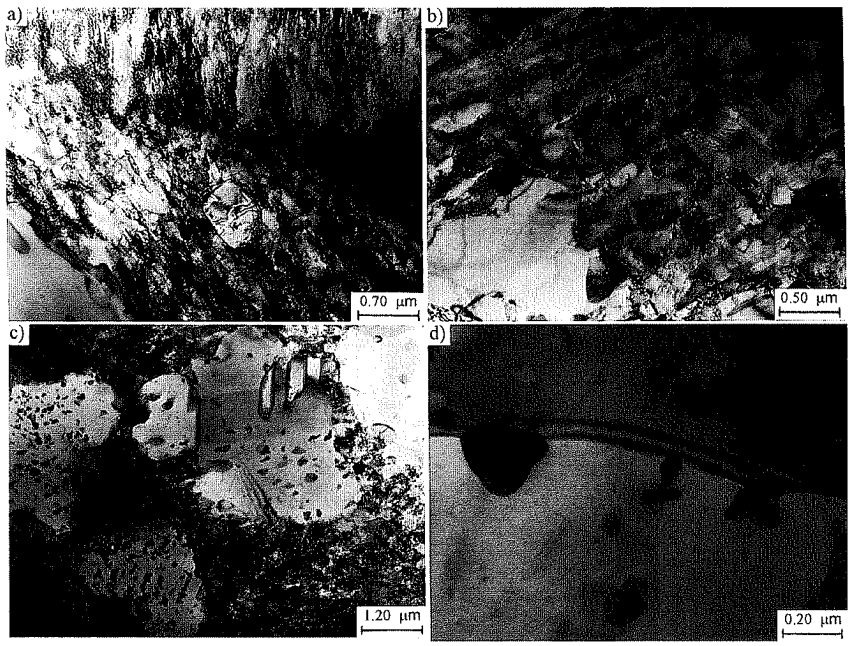

Fig. 6.
TEM bright-field images of different areas throughout the same sample: AISI 304 steel; initially solubilized (S), 60% deformed and annealed at 700°C - 1 h.

carbon in austenitic stainless steels, although increasing the strain hardening and the stored energy due to deformation (driving force for recrystallization), delays the recrystallization. Two possibilities will be analyzed below: carbon in solid solution and carbon in the $(Cr,Fe)_{23}C_6$ form.

The temperatures for 50% softening for the AISI 304L and AISI 304 solubilized at 1 100°C and cold worked to 60% reduction are 700 and 800°C, respectively. For all studied reduction levels (20, 40, and 60%) this behavior repeats, *i.e.*, with higher carbon level there is a higher resistance to recrystallization. In the isochronal curves this reflects itself in differences of about 100°C for a 50% softening. This softening delay can be explained by the $M_{23}C_6$ precipitation during annealing of the supersaturated and cold worked alloys. In general, both austenitic stainless steels show small softening due to recovery, the main softening being caused by recrystallization. An explanation for the small softening due to recovery can be provided by the small SFE of these materials.[9] In materials having low SFE the dislocations have lower mobility, because cross-slip and climb are more difficult.

Figure 6 presents the dislocation substructure (Figs. 6a) and 6b)) and the precipitation of $(Cr,Fe)_{23}C_6$ (Figs. 6c) and 6d)) observed on the TEM in the solubilized AISI 304 steel, cold rolled to 60% and aged at 700°C for 1 h.

The precipitation during annealing of the strain hardened alloys immobilizes the dislocations, the low angle sub-grain boundaries and the high angle grain boundaries, making the recrystallization nucleation difficult as well as the migration of reaction (recrystallization) fronts. This retarding effect is illustrated in Fig. 6d). It is expected that a steel with a higher carbon content available for precipitation (AISI 304) would present higher resistance to recrystallization.

If both steels are compared in the precipitated and strain hardened initial condition, it may be observed that, even in this condition, the material with higher carbon

content shows greater resistance to recrystallization. The precipitation of $(Cr,Fe)_{23}C_6$ in the annealed austenitic stainless steels (not cold worked) occurs preferentially on high angle boundaries. The recrystallization nucleation occurs frequently in the vicinity of grain boundaries. In particular, for austenitic stainless steels, that have low SFE and little tendency to sub-grain formation, the "old" (prior) grain boundaries play an important role on the nucleation of the recrystallization. On the other hand, if high angle boundaries are immobilized by precipitates, the recrystallization should be delayed. In this case, the larger the carbon content of the steel, the greater will be the amount of precipitates and more effective will be the immobilization of the "old" high angle boundaries. On the other hand, the formation of "new" high angle boundaries should not be hindered by the precipitates as in the previous case, since the precipitation occurred during the annealing of the strained supersaturated solid solution.

Comparing in the same steel, for similar conditions of solution annealing and precipitation, it is possible to conclude that the precipitation during the annealing of the strained material is more effective in delaying recrystallization than the precipitation prior to straining. In the isochronal curves, this reflects the differences found of about 50 to 60°C in the 50% softening curves.

The isothermal treatments at 750°C made in samples in the four initial conditions and cold worked to 60% confirm the results obtained in the isochronal treatments (see **Figs. 7a)** to **7d)**). Comparing AISI 304 and AISI 304L, in the initial solubilized condition (Fig. 7a)), it is possible to observe that steel AISI 304 presents higher recrystallization resistance. For example, after 5 min annealing at 750°C, softening was higher than 70% for the AISI 304L, whilst for the AISI 304 softening was less than 30%. Even for the initially precipitated condition, the AISI 304 presented higher recrystallization resistance than the AISI 304L steel (Fig. 7b)). The AISI 304 in the initially solubilized condition presented higher recrystallization resistance than in the precipitated condition. However, in this case, the differences are minor (Fig. 7c)). For example, after 5 min the softening on AISI 304 steel for the initial precipitated condition was about 40% and for the initially solubilized condition was about 30%. For the AISI 304L steel, the differences in the softening behavior in the solubilized and precipitated

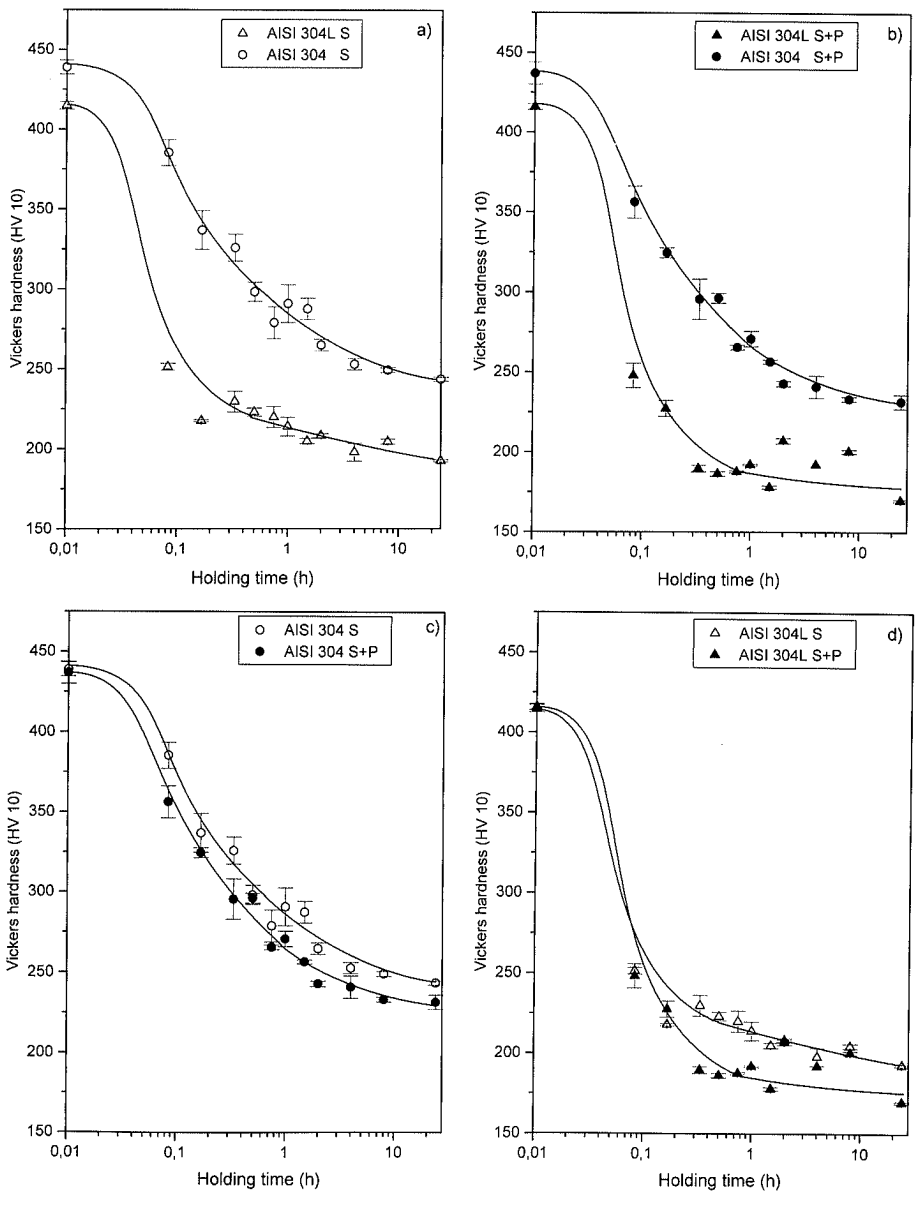

Fig. 7.
Isothermal softening curves (Vickers hardness - 10 kg load *vs.* annealing time at 750°C).
a) AISI 304 and AISI 304L steels; initially solubilized (S) condition.
b) AISI 304 and AISI 304L steels; initially solubilized and precipitated (S+P) condition.
c) AISI 304 steel; initially solubilized (S) and precipitated (S+P) conditions.
d) AISI 304L steel; initially solubilized (S) and precipitated (S+P) conditions.

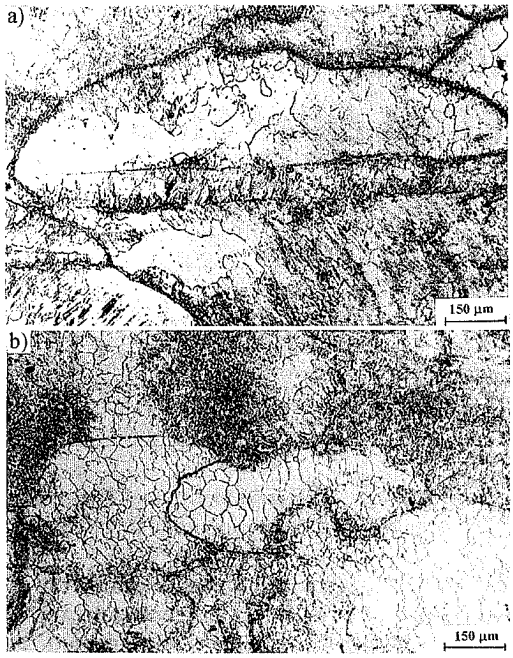

Fig. 8. AISI 304 (8a) and AISI 304L (8b) steels in the (S+P) condition, 60% deformed and annealed at 750°C - 1 h. Optical Microscopy. Electrolytic etching in 30% nitric acid and water. The "old" (prior) grain boundaries were decorated by the $M_{23}C_6$ precipitation.

Table 2. Grain diameter (G.D.) in samples with four different initial conditions after 60% cold working and annealing (950°C - 1 h).

Material	AISI 304L	AISI 304L	AISI 304	AISI 304
Condition	S	S+P	S	S+P
G.D. (μm)	30.9	32.5	28.7	26.9

conditions were even less, as can be seen in Fig. 7d).

Finally, it should be pointed out that it was not possible to establish in this work a simple and direct relation between the α'-reversion and the recrystallization. No precipitation of σ-phase was detected in the range of aging times studied.

3.6. Recrystallized Grain Size

Recrystallization caused a significant grain refinement for the four studied conditions (see **Figs. 8a)** and **8b)**). The microstructures of the samples in Fig. 8 show that they are not fully recrystallized, as shown in Fig. 7b). For a 60% straining, the grain size after recrystallization was practically independent of its initial heat treated condition (see **Table 2)**. Probably for lower strain levels the differences in recrystallized grain size for the four conditions would be more significant. However, a systematic study of this point was not attempted.

3.7. Intergranular Corrosion

The corrosion tests showed that the AISI 304 steel initially solubilized and subsequently recrystallized at 950°C, besides having smaller grain size, was not susceptible to intergranular corrosion. The $(Fe,Cr)_{23}C_6$ precipitation during recrystallization is more uniform and only slightly localized at grain boundaries. Furthermore, even for carbon levels in the maximum allowable level (C<0.08%), the $M_{23}C_6$ carbides are unstable (soluble) at 950°C.[1] These results indicate that the usually employed annealing temperatures (1 000 to 1 120°C) are unnecessarily high. The results of this work indicate that for heavy cold reductions, the temperature range of 950–1 000°C is adequate, because the resulting grain size is smaller and does not affect intergranular corrosion resistance.

4. Conclusions

The experiments performed in this work, the analysis and discussion of the results lead to the following conclusions:

(1) The AISI 304 steel, with %C=0.065, presents higher strain hardening than the AISI 304L steel having %C= 0.021. For the same steel, carbon is more effective in relation to strain hardening when in solid solution.

(2) The AISI 304L steel presented higher tendency to strain induced martensite formation than the AISI 304 steel. The carbon that comes out of solid solution, due to precipitation, led to a greater susceptibility to strain induced martensite in both steels.

(3) The $(Cr,Fe)_{23}C_6$ precipitation modified the composition in the vicinity of grain boundaries, thus affecting the formation of martensite on cooling in the AISI 304 steels, even without strain.

(4) The carbon content in the steel and its condition, in solid solution or in the precipitated form, did not alter significantly the martensite reversion temperature.

(5) The recrystallization nucleation occurred predominantly in the vicinity of grain boundaries.

(6) The steel with higher carbon content presented a higher recrystallization resistance.

(7) The $(Cr,Fe)_{23}C_6$ precipitation during annealing of the solubilized and strained alloys delays the recrystallization, as compared to the situation in which the steel was treated to have precipitation prior to deformation.

(8) The annealing temperatures usually recommended (1 000 to 1 120°C) are unnecessarily high. For example, for the AISI 304 highly strained, a temperature in the range of 950–1 000°C would be more adequate.

REFERENCES

1) M. Deighton: *J. Iron Steel Inst.*, **208** (1970), 1012.
2) E. P. Butler and M. G. Burke: *Acta Metall.*, **34** (1986), 557.
3) D. R. Harries; Proc. of the Int. Conf. on Mechanical Behavior and Nuclear Applications of Stainless Steels at Elevated Temperatures, Metals Society, Varese, Italy, (1981), 1.
4) R. E. Schramm and R. P. Reed: *Metall. Trans.*, **6A** (1975), 1345.
5) R. Fawley, M. A. Quader and R. A. Dodd: *Trans. Metall. Soc. AIME*, **242** (1968), 771.
6) V. Seetharaman: *J. Mater. Sci.*, **16** (1981), 523.
7) A. Weiss, X. Fang, H.-J. Eckstein, C. Eckstein and W. Dahl: *Steel Res.*, **66** (1995), 495.
8) H. Smith and D. R. F. West: *J. Mater. Sci.*, **8** (1973), 1413.
9) S. W. Yang and J. E. Spruiell: *J. Mater. Sci.*, **17** (1982), 677.
10) J. Singh: *J. Mater. Sci.*, **20** (1985), 3157.
11) E. Hornbogen and U. Koster: Recrystallization of two-phase alloys, Recrystallization of Metallic Materials, ed. by F. Haessner, Dr Riederer-Verlag, Stuttgart, (1978), 159.
12) G. Petzow: Metallographisches Ätzen, Gebrüder Bornträger, Berlin, (1984).
13) F. C. Bell and D. E. Sonon: *Metallography*, **9** (1976), 91.
14) T. J. Angel: *J. Iron Steel Inst.*, **177** (1954), 165.
15) J.-Y. Choi and W. Jin: *Scr. Mater.*, **36** (1997), 99.